Multi-Scheme PSK and QAM Modulator Through Vector Scaling and Summation

Shrijeet Mondal[1], Jiangtao Xu[2] and Carlos Saavedra[1]

[1]Dept. of Electrical and Computer Engineering, Queen's University, Kingston, Canada K7L 3N6
[2]Department of Microelectronics, Xian Jiaotong University Xian, Shaanxi Province, China

***Abstract*—A 5.4 GHz direct-digital modulator capable of producing both PSK and QAM modulation schemes is presented. The circuit uses a vector summing approach in which variable-gain OTAs are used to scale the vectors. Vector summation occurs in the current domain and 4-PSK, 8-PSK, 4-QAM and 16-QAM modulation formats are demonstrated. Measurement results on the fabricated circuit show that the highest developed EVM is 8.51% for the 8-PSK modulation scheme. The chip was fabricated at 130nm-CMOS technology and the chip area occupies 0.09 mm^2. The circuit consumes 13 mA and operates at the standard 1.2 V supply for a 130 nm process.**

I. Introduction

In telecommunications, the use of different modulation formats over the same spectrum of operation has lent itself to efficient use of the availed bandwidth. Phase-Shift Keying (PSK) and Quadrature Amplitude Modulation (QAM) are two classic modulation schemes that have given rise to a multitude of different circuits. However, few modulation architectures [2],[3] have attempted to carry out multiple modulation schemes with the same design.

A direct-conversion modulation approach is attractive because of the associated low cost, small chip area and elimination of intermediate frequency (IF) components. Furthermore, a direct-conversion modulator capable of carrying out multiple modulation schemes leads to a greater economy of overall circuit area and increased system versatility. With the emergence of heterogeneous circuits and digital control techniques, a multi-scheme modulator could greatly improve the quality of performance in radio systems with multiple communication standard capability.

A direct-conversion modulator with multiple modulation scheme capability is presented in this paper. The modulator uses a unique design for the orthogonal vector generation, modulation and summing which allows for a large degree of flexibility during its mode of operation. The modulator carries out 4-QAM, 16-QAM, 4-PSK and 8-PSK modulation at an operating frequency of 5.4 GHz with error vector magnitude values of only 2.33%, 6.20%, 3.69% and 8.51% respectively. The results for the QAM modulation schemes were previously reported in [4]. This paper presents the multi-scheme modulation capabilities and the PSK modulation results of the modulator.

II. Circuit Architecture

Figure 1 shows the component-level schematic of the modulator. The modulator has a symmetric structure and is composed of a pair of identical Active Baluns, Operational Transconductance Amplifiers (OTAs) and switching networks. The variable-gain OTAs used in this modulator have a novel design which allows them to offer a high range of gain variance. The details of this particular OTA design have been documented in [1]. The modulator takes a differential input signal which is introduced with a phase offset of 90° using an off-chip phase-shifter. The signal is then decomposed into four orthogonal basis vectors by the active baluns (I+, I-, Q+ and Q- in Figure 1). Each of these signals are offset from each other by 90° over the 360° span of the I-Q plane. The signals then pass through the two OTAs which convert the vectors voltages into vector currents. The switching network is then used to select a quadrant on the I-Q plane by picking two of the four vectors. These two vector currents are finally summed by a trans-impedance amplifier (TIA) to create the desired constellation point at the output. The TIA converts the vector currents to a vector voltage at the output and also provides the aprropriate output load for the OTAs.

III. Vector Manipulation

The modulator has a versatile design which allows the modulator to trace out constellations within a large span on the I-Q plane. The b_0 and b_1 control voltages allow the system to pick two of the four vectors (one on the *I*-axis and the other on the *Q*-axis), as shown in Figure 2a. The b_2 and b_3 are binary values that control the gain of the two OTAs thereby choosing a 'large' or 'small' vector, as shown in Figure 2b. The range of variability over the *I* and *Q*-plane vectors via the four control voltages (b_0, b_1, b_2, b_3) lends the modulator a high degree of flexibility in its operation.

For an *n*-bit $m_n m_{n-1} \ldots m_1 m_0$ signal to be modulated in Figure 1, 4-PSK and 4-QAM modulation is attained by setting b_0 to m_0 and $b_1$equal to m_1; the b_2 and b_3 voltage levels were set to a logic-level high. For 8-PSK modulation, the m_0 and m_1 bits are set to be equal to b_0 and b_1 as in the 4-PSK case. The m_2 bit is set equal to $b_2 = \bar{b_3}$. 16-QAM modulation is similarly achieved by setting $m_0 = b_0$, $m_1 = b_1$, $m_2 = b_2$, $m_3 = b_3$ respectively.

Figure 3 shows the variance of the modulator's gain as a function of the OTA's control voltage (b_2 and b_3). Varying the

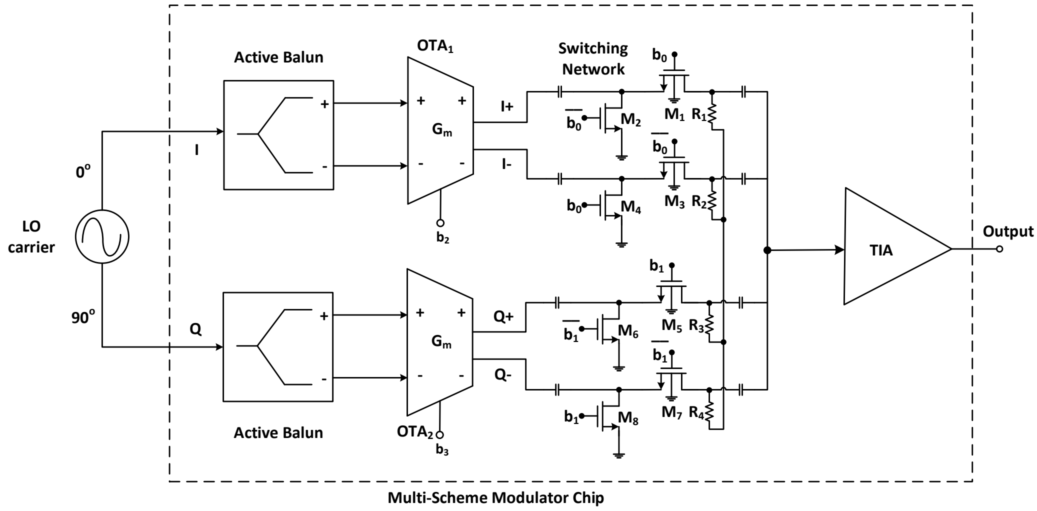

Fig. 1: System-Level Schematic of multi-scheme modulator (taken from [1] with permission © IEEE 2011)

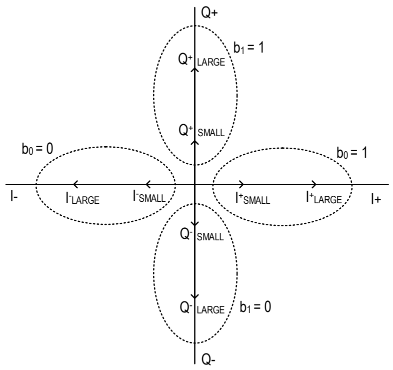

(a)

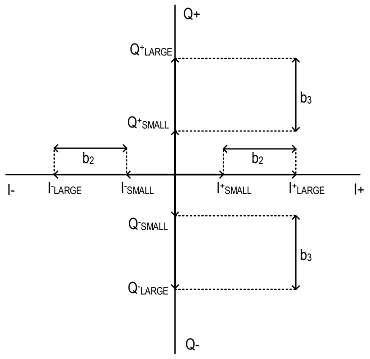

(b)

Fig. 2: (a) Quadrant selection using b_0 and b_1 and (b) Vector magnitude control using b_2 and b_3

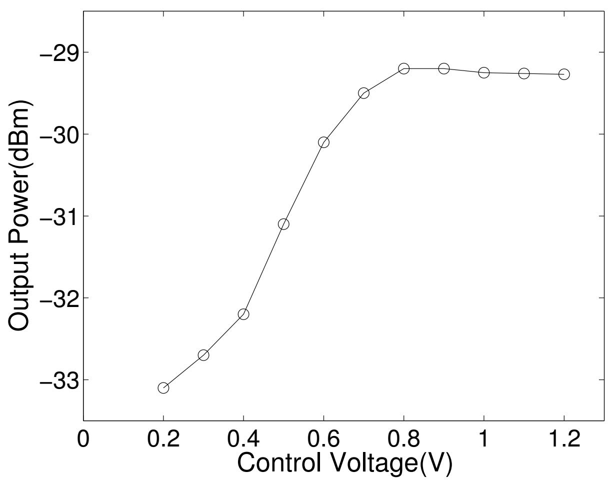

Fig. 3: Variance of output power as a function of the OTA control voltage

b_2 or b_3 voltage from ground to $1.2V$ correlates to a variance in gain of 4dB which is a gain factor of 2.51. The OTA gain range thus limits this design from achieving PSK modulation schemes higher than 8-PSK. Higher modulation schemes may easily be incorporated in future designs with an intermediate transconductance stage with a higher gain.

The maximum *n*-value achieved for the *n*-PSK modulation scheme by the modulator in this work is 8. This value is determined by the range within which the 'large' and 'small' vectors can trace out constellations. In Figure 4a, the larger vector needs to be 2.4 times the smaller vector to trace out the constellation points offset by 45° for 8-PSK modulation. Similarly, for 16-PSK modulation, the larger vector needs to be 5.03 times the smaller vector in magnitude to trace out the required constellation, as shown in Figure 4b.

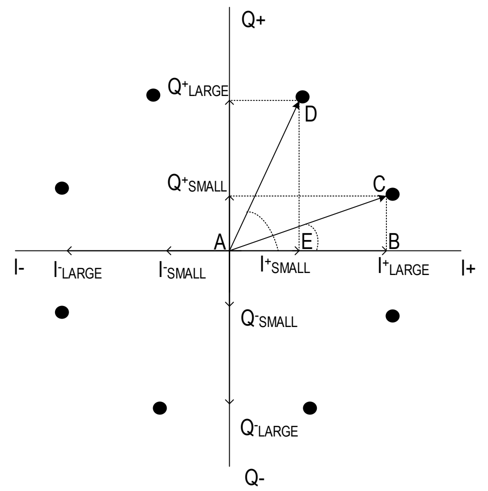

(a)

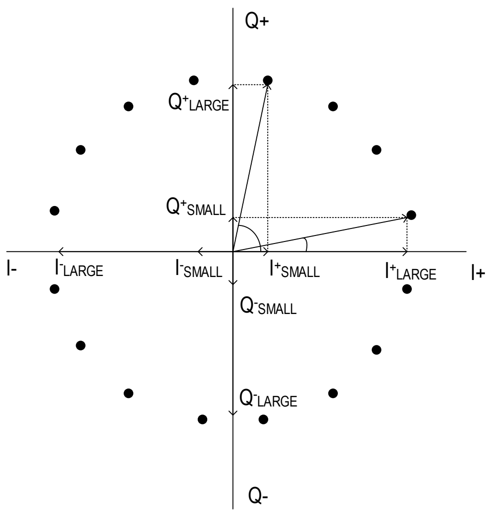

(b)

Fig. 4: (a) 8-PSK and (b) 16-PSK generated using basis vectors

IV. Experimental Results

CPW probes were employed to carry out on-chip measurements. Two Filtronic 6705K tunable phase-shifters were used at the input to attain the 90° phase difference for the RF signal. The phase difference was achieved by setting the phase-shifters at offsets of 30° and 60°. The difference in transmission loss between the two phase shifters was 0.02 dB. Three Tektronix AFG310 function generators were used to generate the pseudorandom bit-sequence. The function generators were synchronized via the trigger-in/out ports to ensure proper transmission of the message signal. The chip was biased using a digital DC supply voltage. The digital demodulation option in an Agilent E4446A Spectrum Analyzer was used to measure the performance of the modulation. For each set of constellations a set of 100 sample constellation points were taken and the results were averaged. Each demodulation scheme was carried out on three chips to account for any manufacturing defects. The output signal power in the 4-PSK mode was -30.8 dBm and in the 8-PSK mode was -28.5 dBm with an input signal power of -22 dBm.

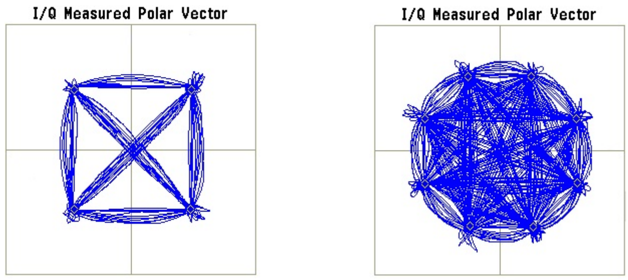

(a) (b)

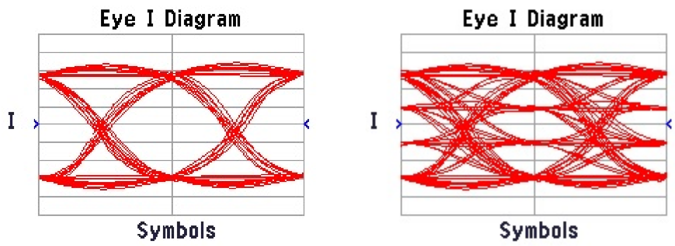

(c) (d)

Fig. 5: (a) 4-PSK constellation, (b) 8-PSK constellation, (c) 4-PSK eye diagram and (d) 8-PSK eye diagram

During 8-PSK modulation, the direct complement for the b_2 value was achieved by using an inverter. The voltage levels for the b_2 and b_3 bits were also stepped down using a voltage divider circuit by a factor of 0.96 to attain the required vector ratio for an 8-PSK constellation.

Figures 5 and 6 shows the output constellation diagrams and eye diagrams for the PSK and QAM modulation schemes, respectively. The QAM results presented were previously reported by Xu and Saavedra in [4]. The constellation graphs confirm that the modulator is effective at carrying out modulation in both modulation schemes effectively. There is an even spread in the number of the paths between each constellation point which confirms that the system is proficient at modulating with pseudorandom data.

Table I shows the EVM of the received signal for different modulation schemes. The highest EVM is developed for the 8-PSK modulation while the lowest EVM is observed during 4-QAM modulation.

TABLE I: EVM for different modulation schemes

	4-PSK	8-PSK	4-QAM	16-QAM
EVM(%)	**3.69**	**8.51**	**2.33**	**6.20**

TABLE II: Performance Summary and Comparison Table

Ref.	Op. Freq. (GHz)	Min. EVM (%)	Reconfigurable? (Y/N)	Max. Mod. Schemes	$P_{consumed}$ (mW)	Chip Area (mm^2)
This Work	5.4	2.33	Y	4	24	0.09
[5]	42	2.5	Y	4	138	5
[6]	2.45	4.95	N	1	12.7	0.02
[7]	5.2	3.7	Y	3	152.5	2
[8]	60	5.5	Y	3	-	2.88
[9]	20-40	< 3	N	1	-	0.38

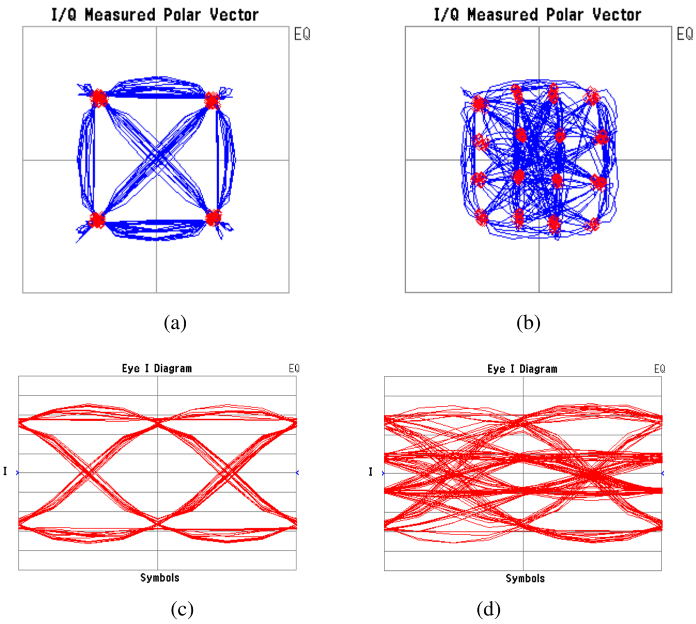

(a) (b) (c) (d)

Fig. 6: (a) 4-QAM constellation, (b) 16-QAM constellation, (c) 4-QAM eye diagram and (d) 16-QAM eye diagram [from [1] with permission ©IEEE 2011]

Table II displays a summary of the metrics of the modulator in comparison to prior work done with other modulators. Compared to other modulators, this modulator displays low EVM values while offering multi-scheme modulation capability, a high data transmission rate and low levels of power consumption.

V. Conclusion

A novel multi-scheme modulator with an operating frequency of 5.4 GHz is presented in 0.13um-CMOS process. The modulator is capable of modulating signals in PSK as well as QAM modulation schemes. The modulator is composed of two OTAs and a switching network which allows for convenient selection and scaling of vectors on the I and Q-planes. Measurement results show accurate constellation points depicting proper modulation of the data with a maximum EVM of 8.51%.

References

[1] J. Xu, C. E. Saavedra, and G. Chen, "Wideband microwave ota with tunable transconductance using feedforward regulation and an active inductor load," in *NEWCAS Conference (NEWCAS), 2010 8th IEEE International*. IEEE, 2010, pp. 93–96.

[2] P.-Y. Tsai, S.-Y. Hsu, J.-S. Chang, T.-W. Chen, and C.-Y. Lee, "A qpsk/16-qam ofdm-based 29.1 mbps linc transmitter for body channel communication," in *Solid State Circuits Conference (A-SSCC), 2012 IEEE Asian*. IEEE, 2012, pp. 345–348.

[3] A. Seyedi, "Multi-qam modulation: A low-complexity full-rate diversity scheme," in *Communications, 2006. ICC'06. IEEE International Conference on*, vol. 4. IEEE, 2006, pp. 1470–1475.

[4] J. Xu, C. E. Saavedra, and G. Chen, "5.4 ghz reconfigurable quadrature amplitude modulator using very high-speed otas," in *Microwave Symposium Digest (MTT), 2011 IEEE MTT-S International*. IEEE, 2011, pp. 1–4.

[5] A. K. Gupta and J. F. Buckwalter, "Linearity considerations for low-evm, millimeter-wave direct-conversion modulators," *Microwave Theory and Techniques, IEEE Transactions on*, vol. 60, no. 10, pp. 3272–3285, 2012.

[6] T. van Zeijl Paul and M. Collados, "A digital envelope modulator for a wlan ofdm polar transmitter in 90 nm cmos," *Solid-State Circuits, IEEE Journal of*, vol. 42, no. 10, pp. 2204–2211, 2007.

[7] S. Gueorguiev, S. Lindfors, and T. Larsen, "A 5.2 ghz cmos i/q modulator with integrated phase shifter for beamforming," *Solid-State Circuits, IEEE Journal of*, vol. 42, no. 9, pp. 1953–1962, 2007.

[8] Y. Hamada, K. Maruhashi, M. Ito, S. Kishimoto, T. Morimoto, and K. Ohata, "A 60-ghz-band compact iq modulator mmic for ultra-high-speed wireless communication," in *Microwave Symposium Digest, 2006. IEEE MTT-S International*. IEEE, 2006, pp. 1701–1704.

[9] H.-Y. Chang, P.-S. Wu, T.-W. Huang, H. Wang, C.-L. Chang, and J. G. Chern, "Design and analysis of cmos broad-band compact high-linearity modulators for gigabit microwave/millimeter-wave applications," *Microwave Theory and Techniques, IEEE Transactions on*, vol. 54, no. 1, pp. 20–30, 2006.

[10] H.-o. Ueda, K. Nakajima, G. Kanazawa, M. Shimozawa, J. Koide, M. Uesugi, R. Takeuchi, N. Suematsu, Y. Isota, S. Kameda *et al.*, "A 5ghz-band sige-mmic transceiver for 324mbps transmission," in *Radio and Wireless Symposium, 2008 IEEE*. IEEE, 2008, pp. 791–794.

[11] D. M. Pozar, *Microwave engineering*. John Wiley & Sons, 2009.

[12] K. Nakajima, T. Sugano, and N. Suematsu, "A 5 ghz-band sige-mmic direct quadrature modulator using a doubly stacked polyphase filter," in *Radio frequency integrated circuits (RFIC) symposium, 2004. Digest of papers. 2004 IEEE*. IEEE, 2004, pp. 409–412.

[13] Y. Zheng and C. E. Saavedra, "Feedforward-regulated cascode ota for gigahertz applications," *Circuits and Systems I: Regular Papers, IEEE Transactions on*, vol. 55, no. 11, pp. 3373–3382, 2008.